Morphology study for carbon nanostructered iron catalysts based on the difference in the gaseous medium and the thermal treatments

Mai M. Khalaf*, H.C.Ibrahimov, E.H.Ismailov, Y.H.Yusifov and N.M.Alieva

Institute of Petrochemical Processes, Azerbaijan National Academy of Sciences 30, Khojaly Ave., Baku,

AZ1025, Azerbaijan,

*Chemistry Department, Faculty of Science, Sohag University, 82524 Sohag, Egypt

Email: mai_kha1@yahoo.com

Abstract: The special features of nano-structured materials have been motivating the search for new synthesis methods for these types of materials. This paper is concentrated on the characterization of carbon nanostructured materials containing iron ions synthesized by a new method based on the reaction of fine-dispersed Al flakes with dichloroethane in paraffin medium in the presence of iron chloride forming catalytic complexes at different calcined temperatures, and at different gaseous medium. This chemical-based synthesis route is briefly described, and the feasibility of obtaining such systems. Characterization was done by X-ray fluorescence microscopy (XRFM), X-ray diffractometer (XRD), which revealed, respectively, the presence of oxides and their nanoscale structures, including the elemental distribution and mass thickness of the these elements over the layers . In addition, the surface morphology of these complexes was also conformed by N2 adsorption analyses and scanning electron microscope (SEM).

Key word: N2 adsorption isotherms, XRFM, Fe/CTC, XRD, SEM

Introduction:

Nanostructured materials exhibit different, often enhanced, magnetic, electronic, optical and reactive properties compared to corresponding bulk materials, making them desirable for applications including catalysis, adsorption, ferrofluids, electronic sensing, medical applications, and drug delivery [1–6]. In order to enhance the catalytic activity and stability of these materials, different combinations of these active metals have been reported such as Co-Fe [7], Co-Mn [8] and Fe-Mn [9]. The performance of these catalysts is affected by numerous factors, one of which is the nature and structure of the support materials. Tiny particles of iron oxide could become tools for simultaneous tumor imaging and treatment, because of their magnetic properties and toxic effects against brain cancer cells. Iron oxides play an important role in wastewater treatment adsorbents. The high versatility and structural chemistry variability of iron oxide is a result of the existence of two oxidation stable states for iron, ferrous ions (Fe^{+2}) and ferric ions (Fe^{+3}) in a wide range of pH and the condensation phenomenon [10–13]. Iron oxides in nano-scale have exhibited great potential for their applications as catalytic materials, pigments, flocculants, coatings, gas sensors, ion exchangers, magnetic recording devices, magnetic

data storage devices, toners and inks for xerography, magnetic resonance imaging, bio separation and medicine. Nano sized magnetite Fe_3O_4, and maghemite γ-Fe_2O_3 exhibiting excellent magnetic properties find applications for biomedical purposes and as soft ferrites. In catalysis both iron oxides and hydroxides find application in numerous synthesis processes. Also $FeAl_2O_4$ phase provides an excellent combination of physical and chemical properties [14]. Iron is a widely used catalyst for the growth of carbon nanotubes (CNTs) or carbon nanofibers (CNFs) by catalytic chemical vapor deposition. However, both Fe and Fe–C compounds (generally, Fe_3C) have been found to catalyze the growth of CNTs/CNFs [15]. A novel process for the preparation of carbon nanostructured materials with controlled topology, morphology and functionality is discussed. This process based on the reaction of fine-dispersed Al flakes with dichloroethane in paraffin medium in the presence of iron chloride as amodifier. Compositional control over the system provides control over the structure of the phase separated precursor whose organization therein dictates the nanostructure of the material obtained during the process, and the surface characterization of the resulted systems after changing the of gaseous medium and the thermal treatment. In the present study we discussed the introduction of metals in the catalytic complex CTC with the direct participation of the metal salts in the reaction, resulting in formation of bimetallic complex of the type Fe/CTC. Bulk and surface characterization of the formation of metal-carbon structures of various dimensions are extremely important, because having these results, it is possible to develop a directed synthesis methods of metal-carbon structures required composition. The nanostructured carbon materials modified with iron chloride are confirmed by different techniques, such as X-ray fluorescence microscopy (XRFM), X-ray diffractometer (XRD), N_2 adsorption–desorption analysis and scanning electron microscope (SEM).

Experimental

2.1. Preparation

2.1.1. Chemicals

1,2-dichloroethane($C_2H_4Cl_2$),   99.5%   Sigma-Aldrich; Aluminium flakes, 99.99% Aldrich; Heptane (C_7H_{16}), 99% Aldrich; Anhydrous Aluminium chloride($AlCl_3$), 99% Sigma-Aldrich; Iron (III) chloride hexahydrate ($FeCl_3.6H_2O$), 99% Sigma-Aldrich; analytical grade products were purchased and used as received.

2.1.2. Synthesis of Carbon nanostructured materials containing Fe [III] ions in air

Carbon nanostructured materials containing Fe [III] ions in air were synthesized as a catalytic complex CTC modified with metal chloride of Fe (III) [16] in laboratory conditions under atmospheric pressure in a solvent in the mode of «in situ», at a certain ratio of initial components in a round bottom flask (reflux system) at 80-90 $^{\circ}$C for 22-25h. The obtained gel was cooled and aged in the mother liquor at room temperature for 24 h. After that, the solvent was removed under vacuum, and a final drying was carried out at 100-110 $^{\circ}$C. The obtained dried xerogel (designated as Fe/CTC-110) was submitted to thermal treatment at 600, and 850 $^{\circ}$C for 2h, 4h in air, furnishing the materials designated as Fe/CTC-600 2h and Fe/CTC 850 4h.

2.1.2. Synthesis of Carbon nanostructured materials containing Fe [III] ions in inert atmosphere

Carbon nanostructured materials containing Iron catalyst in inert atmosphere were synthesized also as catalytic complex Fe/CTC, and deposited in a MPCVD system (MPCVD75-3 CVD nanocarbon generation equipment).

Vacuum was supplied by a combination of a turbo-molecular pump and a rotary pump. Working gases (C_2H_2 and He) were fed into the deposition chamber through mass flow controllers. Pressure in the chamber was controlled by adjusting a valve between the deposition chamber and the vacuum pump. The power of microwave in the chamber was adjusted by a four screw adapter and monitored by measuring the back reflection power at the end of water load. Temperature is determined by the power of microwave in the deposition chamber, the flow rates of working gases, working pressure and the position of substrate in the deposition chamber. The substrate temperature ranges from 700 to 800 $^\circ$C, and the working pressure is about - 0.095 MPa. The flow rates of C_2H_2 and He are about 20 and 100 ml/min respectively. The sample was deposited for one hour and has a thickness of a few hundred of nanometers. The deposition rate is about 2–6 nm/min depending on growth condition. The resulted sample is designated as Fe/CTC-800 He

2.2. Characterization techniques

2.2.1. X-ray fluorescence microscopy (XRFM)

Elemental analysis of the samples were performed by using X-ray microscope XGT-7000, Horiba with accelerating voltage of X-ray tube 50KV, the diameter of the incident X-ray beam was 100 microns, and the measurement time was 200 sec. the samples were crushed to powder and pressed. The Full Vacuum mode was used which provides elemental analysis for light elements such as aluminium, with the sample chamber maintained at normal atmospheric pressure.

2.2.2. X-ray diffractometer (XRD)

XRD patterns were obtained using TD-3500 diffractometer at room temperature. Diffraction patterns were obtained with none-filtered Cu Kα radiation (λ = 0.15418 nm), monochromatic X-ray beam, and X-ray tube parameters with 35 kv and 25 μA.

2.2.3. N2 adsorption–desorption analysis

N_2 adsorption–desorption isotherms at -196 $^\circ$C were obtained with a NOVA 3200 apparatus, USA. The samples were previously out gassed under a reduced pressure to 0.1 pa at 200 $^\circ$C for 2 h. Specific surface areas (S_{BET}) were calculated from multi-point at relative pressure (P/P_0) ranging from 0.05 to 0.30. Pore size distribution curves were obtained from Barrett, Joyner and Halenda (BJH) method using the adsorption branch of the isotherms. Assessments of microporosity were made from t-plot constructions, using the Harkins-Jura correlation.

2.2.4. Scanning electron microscopy (SEM)

In order to observe any changes in surface morphologies of the samples, the specimens were analyzed by using scanning electron microscope (JEOL, model 5300).

Results and discussion

3.1. Nitrogen Adsorption/desorption Results

 3.1.1. Isotherms and total pore volume

Low temperature adsorption–desorption isotherms of N_2 for Fe/CTC-600 in air for 2h, Fe/CTC-850 for 4h and Fe/CTC-800 in He for 1 h samples are illustrated in Fig. 1. Derived surface data are included in Table 1. All the obtained isotherms of similar isotherm profiles characteristic to type IV at high relative pressures (p/p_o), typical of mesoporous materials according to IUPAC classification **[17],** with type H1 hystersis loops, for all samples

and type I of isotherm which characteristic to the micropore filling process of N_2 sorption **[18]** with type H4 hystersis loops for the Fe/CTC at 800 °C in He. The increasing of calcined temperatures during the thermal treatment could not affect largely the shape of the adsorption isotherm from 600 to 850 °C, and slightly changed for this group at 800 °C in inert atmosphere (He) as a result of changing the gaseous medium. BET specific surface area, total pore volume and average pore diameter of the samples are listed in Table 1 and the S_{BET} of can be calculated from the slop of the BET relation as shown in Fig. 1.

There was a significant decrease in BET specific surface area and pore volume for Fe/CTC at 850 °C than at 600 °C in air. Specific surface areas, S_{BET}, of Fe/CTC 600 2h, and Fe/CTC 850 4h in air were found to be 153, 78.3 m^2 g^{-1}, respectively, while its pore volume were 0.3767, 0.3375 cm^3 g^{-1}. The decrease in BET specific surface area (reduced by 48%) and total pore volume when switching from calcinations at 600 °C to 850 °C indicated that Fe nanoparticles were mainly incorporated inside the pores rather than on the external surface of Fe/CTC at 850 °C for 4 h. This effect was due to the presence of the mixed phases of iron oxides at 600 °C for 2 h as discussed in XRD studies. The surface area and total pore volume was obtained for Fe/CTC after thermal treatment at 800 °C in inert atmosphere (He) S_{BET}, was amounting to 208 m^2 g^{-1}. Total pore volume, V_p, amounting to 0.1351 cm^3 g^{-1} for the same reasons.

3.1.2. t-plot

t-plot for Fe/CTC-600 in air for 2h is shown in Fig. 2. S_{mic} value amounting to 55.9 m^{2}g^{-1} (out of S_{BET} = 153).This indicates the presence of mesoporosity for the catalytic complex modified with iron and thermally treated at 600 °C for 2 h, and the data obtained from this analysis were cited in Table .1. *t*-plot for the catalytic complexes of Fe/CTC after thermal treatment at 850 °C for 4 h in air is shown in Fig. 3, the values of microporosity, S_{mic}, amounting to 16.4 m^{2}g^{-1} (out of S_{BET} = 78.3 m^{2}g^{-1}).Results indicated that small values of microporosity, S_{mic}, whereas, mesoporous porosity was detected for Fe/CTC materials after thermal treatment at 600, 850 °C for 2, 4 h in air.

t-plots for the catalytic complexes of Fe/CTC after thermal treatment at 800 °C in inert atmosphere (He) is shown in Fig. 4 Results indicated values of microporosity, S_{mic}, amounting to 102.9 m^{2}g^{-1} (out of S_{BET} = 208 m^{2}g^{-1}). This indicates that after thermal treatment at 800 °C in inert atmosphere (He) for these catalytic complexes modified with Fe and Co chlorides help the formation of mixed surface with micro and mesoporous porosity.

3.1.3. Pore size distributions

Pore width, PWD, distributions obtained with the catalytic materials modified with iron calcined at 600 °C for 2 h, at 850 °C for 4 h in air and at 800 °C in He are shown in **Fig.** 5, The BJH pore width, PWD, maximizing at 8.1 nm for Fe/CTC-600 in air 2 h. and at 800 °C in He, PWD,maximizing at 2.4 nm. This indicates that mono sized distribution obtained with these cases. However, at 850 °C for 4 h in air maximizing at ~ 14 nm, another peak was developed at ~ 35 nm, this bidistribution confirmed the same result of the decreasing its surface area.
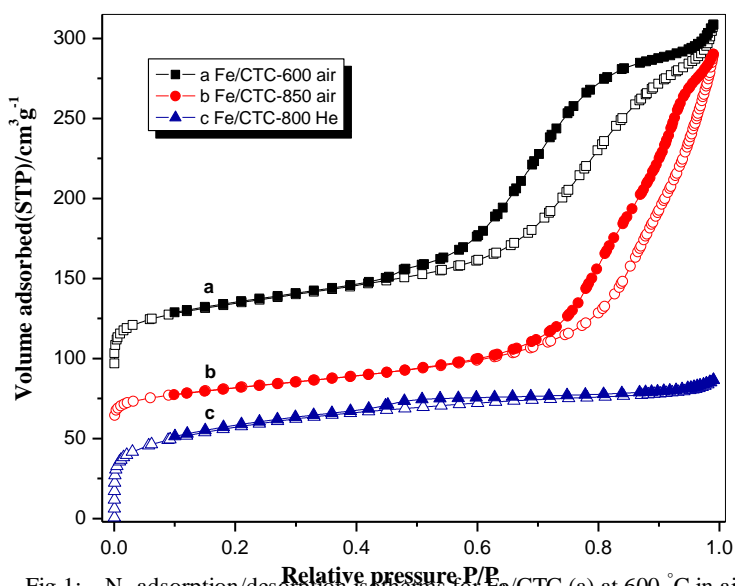
Fig.1: N_2 adsorption/desorption isotherms for Fe/CTC (a) at 600 °C in air for 2h (b) at 850 °C in air for 4h (c) at 800 °C in He

Table 1: Textural characteristics for calcined samples of CTC modified with Fe in air atmosphere for 2h, 4h and in inert atmosphere (He)

Samples	C_{BET}	S_{BET} / m^2g^{-1}	V_p/cm^3g^{-1}	t-method m^2g^{-1}		Pore width W_p/ nm	
				S_{mic}	S_t	4V/ S_{BET}	BJH
Fe/CTC-600 2h	215.2	153	0.3767	55.9	97.1	9.1	8.1
Fe/CTC-850 4h	109.4	78.3	0.3375	16.4	61.9	15.3	13.9
Fe/CTC-800 He	123.2	208	0.1351	102.9	105.1	3.9	2.4
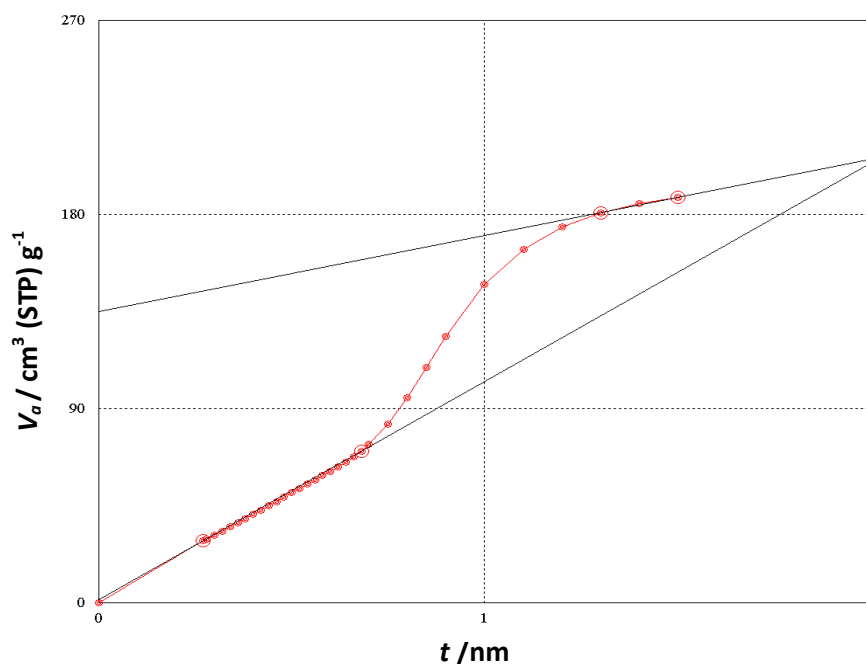
Fig.2:   t-plot for Fe/CTC-600 in air for 2h
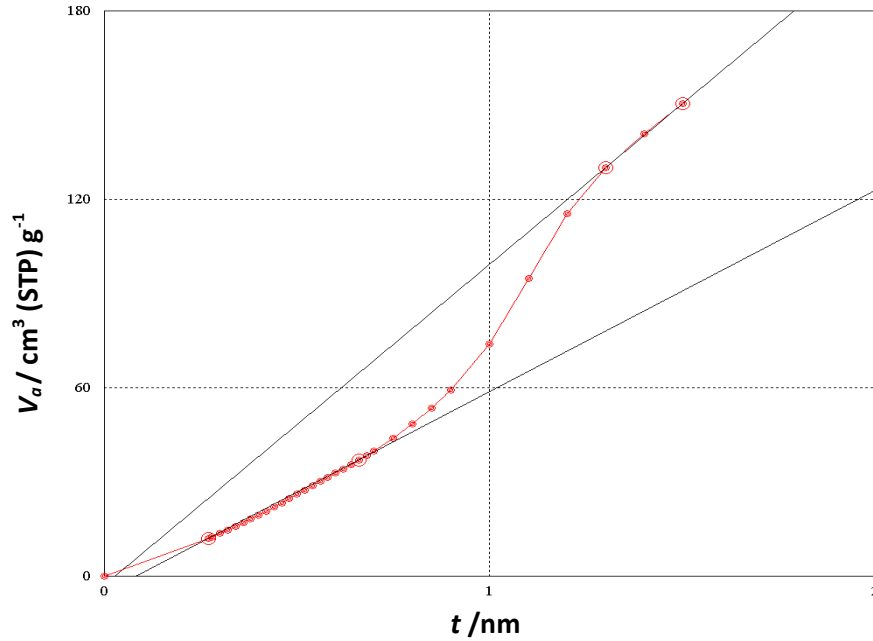
Fig.3:   t-plot for Fe/CTC-850 in air for 4h
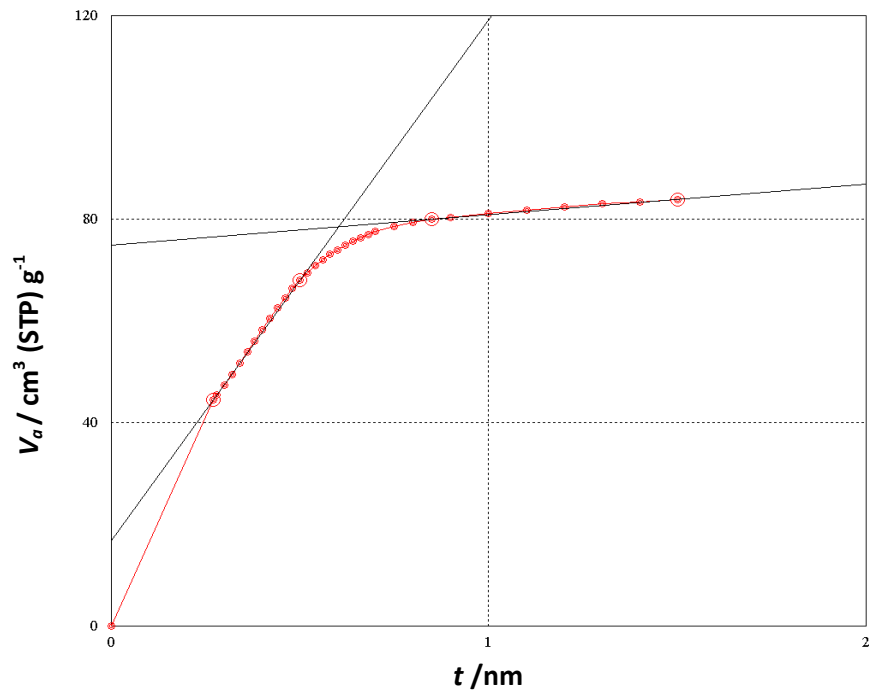
Fig. 4:   t-plot for Fe/CTC-800 in He

3.2. X-ray fluorescence microscopy (XRFM) characterization

For samples after calcinations at 600,850 °C for 2h in air as shown in Table 2, the aluminate, AlO_2^- tetrahedral complex that is negatively charged and iron (II) aluminate, Al_2FeO_4 phases were formed, respectively. The

percentage of the chemical composition of the samples given in oxides at different calcined temperatures has not a distinct behavior; it depends on the stability of oxides. The distribution of the Fe element over depth at the different calcined temperatures is higher than that of Al element that is for the higher synthetic ratio of iron and cobalt chlorides rather than Al flakes. There is no change in the chemical compositions and the distribution of elements for the investigated samples after calcinations at 600 $^{\circ}$C, this means that the formed oxides at this temperature of higher stability. Also we observed the percentage of the chemical composition of Fe_xO_y for the Fe/CTC complex decrease in the case of calcination for 4h than those obtained after 2h. This due to, the Fe/CTC complex formed mixed oxides of iron in the case of calcination for 2h, but after 4 hours the stable oxide of iron was remained which was confirmed by surface analyses . From the optical image (Fig 6) it was observed that the color of the complex changed by changing in the formed phases.   These results were confirmed by XRD which will be discussed later.
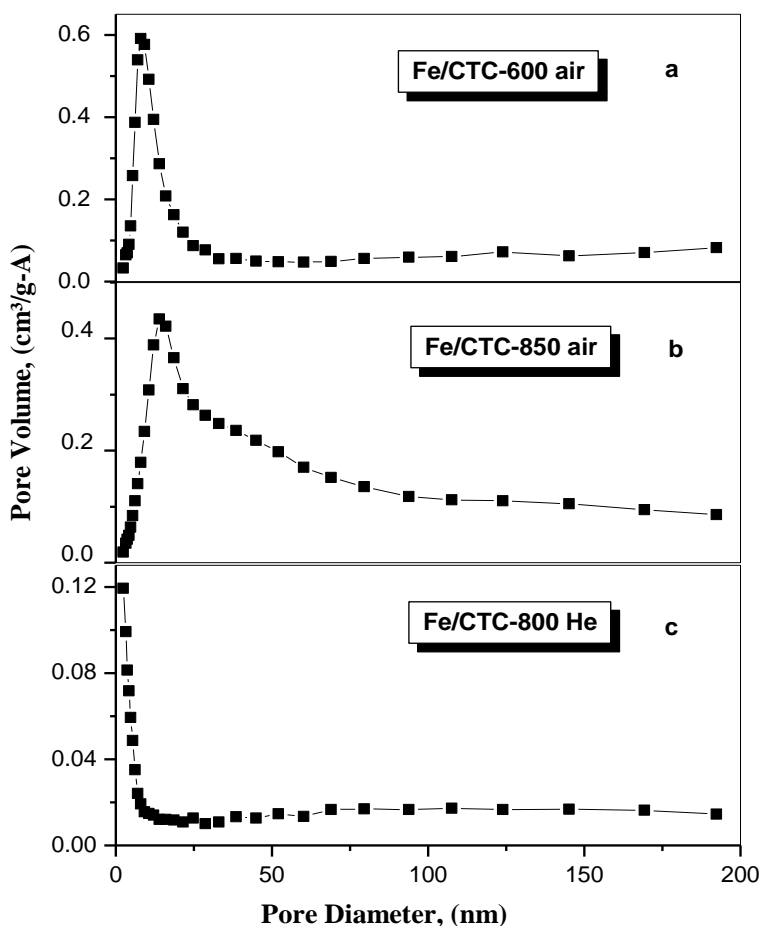
Fig.5:   Pore size distribution for Fe/CTC (a) at 600 $^{\circ}$C in air for 2h
(b) at 850 $^{\circ}$C in air for 4h (c) at 800 $^{\circ}$C in He

For samples after thermal treatments at 800 $^{\circ}$C in inert atmosphere (He) for one hour as shown in Table 3, the iron aluminide, Fe_3AlC_x was formed (Fig. 7). For the volatile and ash percentages of the samples at 800 $^{\circ}$C have almost the same percent that is refers to the reaction conditions. The data in Table 3 showed that, the elemental percentage of carbon for the carbon nanostructured iron catalyst (as Fe/CTC) treated at 800 $^{\circ}$C is higher than

that obtained for samples treated at 600 and 850 °C (Table 2); due to the change in the gaseous medium from air to the inert atmosphere(He).

Table 2:   The elemental and chemical composition of the samples and their distribution of elements over the depth after calcinations in air: 600,850 °C for 2 h and 4 h

samples name	Chemical composition (wt. %)			Elements (wt. %)					Volatile %	Ash %	The distribution of elements over the depth		
	Al$_x$O$_y$	Fe$_x$O$_y$	Cl	Al	*C	Fe	O	Cl			Al	Fe	Cl
Fe/KTK-600 2 h	34.9	64.2	0.9	17.9	3,9	43.6	34.6	0.8	63.2	36.8	0.038	0.773	-
Fe/KTK-850 2 h	66.5	33.5	-	33.8	3.9	22.5	39.7	-	57.5	42.5	0.175	0.267	-
Fe/CTC-600 4 h	82.3	17.9	-	41.8	3.9	12.0	42.3	-	71.8	28.2	0.02	0.032	-
Fe/KTK-850 4 h	82.2	17.8	-	41.8	3.6	12.0	42.3	-	73.5	26.5	0.014	0.027	73.5

*C content was determined by the balance of the treatment of the samples at 600, 850 °C in air for 2 h, 4 h.

Table 3:   The Content of elements (wt. %) in samples treated at 800 °C for 1 hour in inert atmosphere (He) and their distribution over the depth

samples name	Elements (wt. %)				Volatile %	Ash %	The distribution of elements over the depth		
	Al	*C	Fe	Co			Al	Fe	Co
				800 °C					
Fe/KTK-800	12.4	30.2	57.4	-	50.7	49.4	0.007	0.218	-
Co/KTK-800	19.9	34.7	-	45.4	54.9	45.1	0.006	-	0.096

*C content was determined by the balance of the treatment of the samples at 800 °C in He.
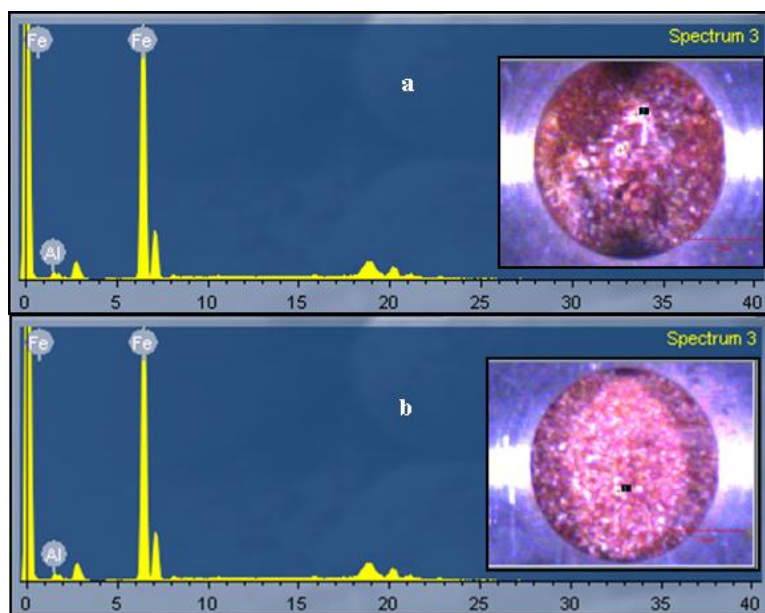
Fig. 6:   EDRF analysis and optical image of (a) Fe/CTC-600

(b) Fe/CTC-850 for 2h in air
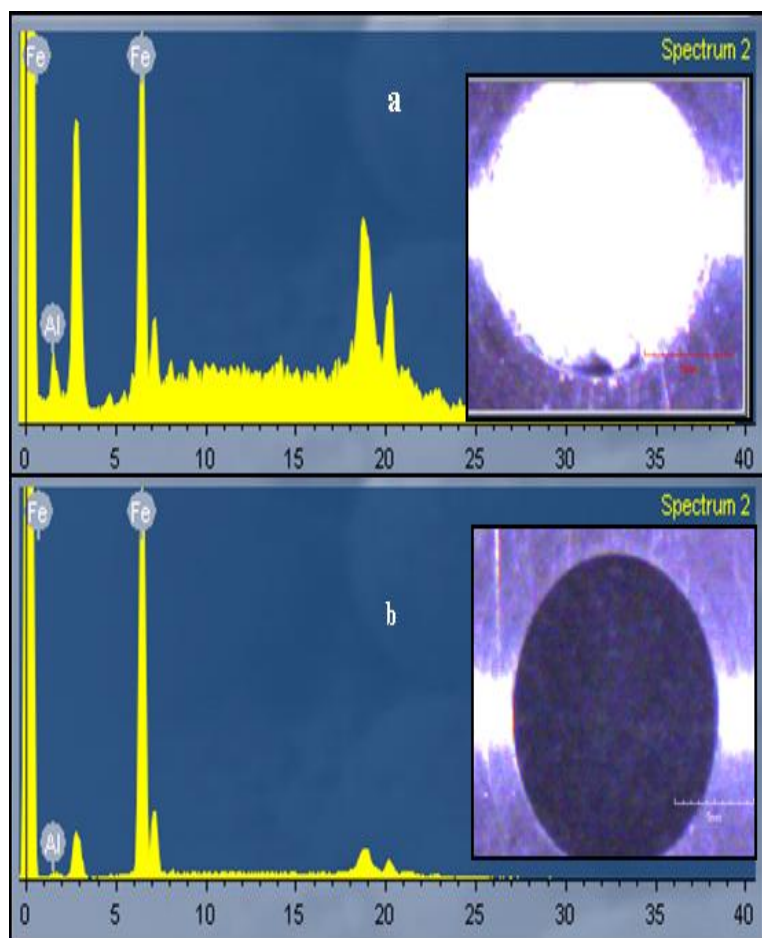
Fig. 7:   EDRF analysis and optical image of Fe/CTC (a) at 850 °C in air for 4 h

(b) at 800°C in He

3.3. X-ray diffractometer (XRD) characterization

Wide angle XRD, WAXRD patterns for the catalytic complex Fe/CTC obtained with thermal treatment at 600 °C for 2h in air, small angle XRD, SAXRD patterns of the same set of materials are inserted. Crystalline phases were obtained as shown in Fig. 8. The cubic Al_2O_3 was obtained for Fe/CTC mixed phases of iron oxides FeO (2θ=61), synthetic magnetite $Fe^{+2}Fe^{+3}O_4$ (2θ=35) and synthetic hematite Fe_2O_3 (2θ=23, 33, 49, 54 and 64) files no. 06-0711, 19-0629 and 33-0664. Also the iron aluminates, $Fe^{+2}Al_2O_4$ phase was formed for the Fe/CTC after calcinations at 850 °C for 2h, and there are peaks at 2θ=31, 37, 58, and 65) file no. 34-0192 were obtained.

For the same group of materials after thermal treatment at 600 °C for 4h in air the phase of synthetic maghemite-c Fe_2O_3 was obtained for Fe/CTC file no. 39-1345. Cubic Al_2O_3 (file no. 29-0063) was formed for Fe/CTC-850 (Fig. 9) for 4h in air, and also Rhombohedral Fe_2O_3 (file no. 33-0664) with characteristic peaks at 2θ= 34, 41 and 62. The

intensity of these peaks increases by increasing the calcined temperatures and by increasing the time of holding these complexes at the investigated temperature.
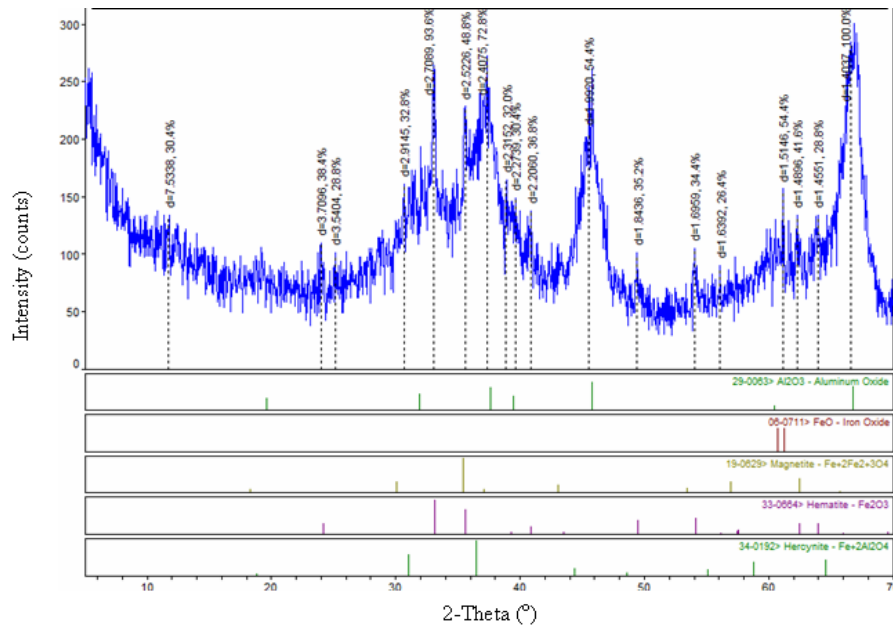
Fig. 8: XRD patterns of Fe/CTC at 600 °C in air for 2h
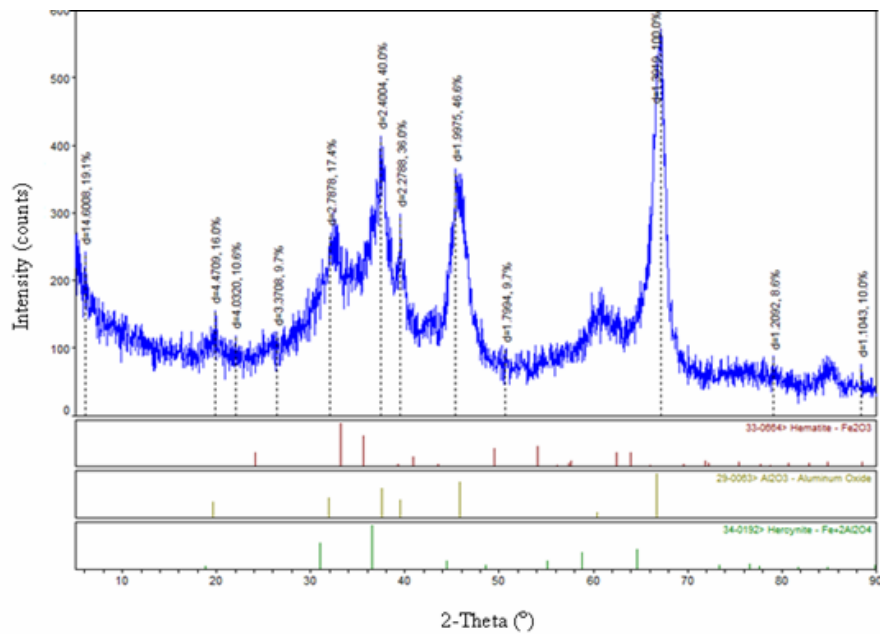
Fig. 9: XRD patterns of Fe/CTC at 850 °C in air for 4h

3.4. SEM analysis

SEM analysis of the prepared catalysts(Fe/CTC, Co/CTC) thermally treated at 850 $^{\circ}$C in air reveals that all the samples showed a nanostructure, the synthesized iron nanoparticles (Fig.10) are ranged in size from 50-100 nm with calculated average size of 100 nm. There is a mixture of nanoparticles of iron with spherical shape and aluminum oxides with rhombic shape and with different particle size as referred in images. The SEM images of Fe/CTC at 800 $^{\circ}$C in He are presented in Figure 11, and have shown the major differences in their morphology in comparison with their counterparts at 850 $^{\circ}$C in air, the particle size of some grains as illustrated in Fig.11 has increased and revealed structural differences, which are probably due to the presence carbon nanoparticles. This formed catalytic systems comprised large grains, which were embedded in a mixture consisting of small grains. However, the size of these grains grew larger by agglomeration at this higher temperature.
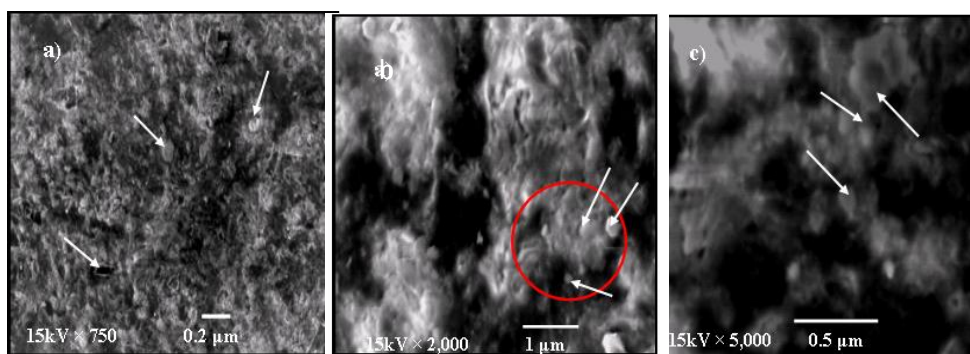
Fig.10: SEM micrographs of samples of Fe/CTC at 850 ◦C in air for 4h at different magnifications
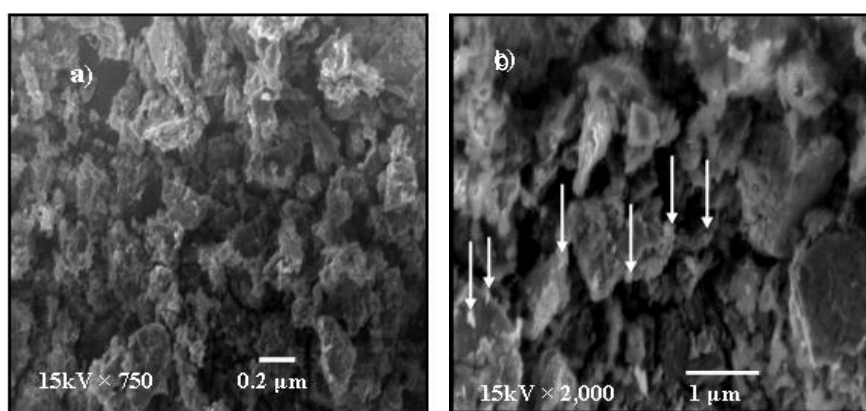
Fig.11: SEM micrographs of Fe/CTC at 800 ◦C in (He) at different magnifications

Conclusions

This paper discussed process for preparing unique carbon nanostructured iron systems as catalytic complex of Fe/CTC at different gaseous mediums and temperatures. This process requires only thermal treatments of these materials in air and in inert atmosphere and uses low cost starting materials. Surface investigation of different samples under study from the N_2 adsorption analyses confirmed the effect of temperature, hold time of Fe/CTC at different time and different gaseous mediums can affect the value of the specific surface area and the total pore volume, this catalytic complex modified with Fe chloride help the formation of mesoporous materials even with holding this complex for four hours at higher temperatures in air. In inert atmosphere we obtained mixed surface of micro and mesoporous porosity. From the previous results it can be observed that modification of the catalytic complex (CTC) with iron chloride give the highest S_{BET} value and total pore volume, V_t value after thermal treatment at 600 °C in air for 2h and after thermal treatment at 800 °C in inert atmosphere (He). From XRFM analyses the difference in the color of carbon nanostructured iron catalyst as Fe/CTC complex from black color at 800 °C in inert atmosphere (He), and mixed color (black and brown) at 600 °C, then brown color at 850 °C for 2h after that light brown color at 850 °C for 4h, this difference confirmed the formation of the different mentioned oxides. The XRD results also proved that by increasing time hold, and calcinations temperatures reduced the resulted phases and lead to increase the intensity of XRD peaks, and this attributed to the increase in the degree of ordering of the particles. It can be more specifically from the SEM results that, higher calcinations temperatures resulted in crystallite growth and agglomeration for samples treated in air, however for the samples treated in inert atmosphere (He) confirmed the presence of carbon nanoparticles .

References

[1]   Enthaler S., Junge K., Beller M., *Su stainable metal catalysis with iron: from rust to rising star*. Angew Chem Int Ed Engl. (2008). vol. 47. pp. 3317.

[2]   Giasuddin A.B.M.,.Kanel S.R. , Choi H., *Adsorption of humic acid onto nanoscale zero valent iron and its effect on arsenic removal. Environ Sci Technol*. (2007) vol. 41.pp. 2022.

[3] Wu K.T., Kuo P.C., Yao Y.D., Tsai E.H., Magnetic and optical properties of Fe_3O_4 nanoparticle ferrofluids prepared by coprecipitation technique. *IEEE Trans Magn*. (2001) vol. 37. pp. 2651.

[4] Shipway A.N., Katz E., Willner I., Nanoparticle arrays on surfaces for electronic, optical, and sensor applications. Chemphyschem. (2000). vol. 1. pp. 18.

[5] Tran N., Pareta R., Taylor E., Webster T.J., Iron oxide nanoparticles: novel drug delivery materials for treating bone diseases. *Adv Mater Res*. (2010) vol. 89. pp. 411.

[6] Chertok B., Moffat B.A., David A.E., Yu F., Bergemann C., Ross B.D., Iron oxide nanoparticles as a drug delivery vehicle for MRI monitored magnetic targeting of brain tumors. Biomaterials. (2008) vol. 29. pp. 487–96.

[7] Arcuri K.B., Schwartz H., Pitrowski R.D., Butt J. B. , Iron alloy Fischer-Tropsch catalysts: IV. *Reaction and selectivity studies of the Fe Co system. J Catal*. (1985) vol. 85. pp. 349.

[8] Morales Cano F., Gijzeman O. L. J., de Groot F. M. F., Weckhuysen B.M., Manganese promotion in cobalt-based Fischer-Tropsch catalysis. Stud in Surf Sci Catal. (2004) vol. 147. pp. 271.

[9] Yang Y., Xiang H., Zhang R., Zhong B., Li Y., *A highly active and stable Fe-Mn catalyst for slurry Fischer-Tropsch synthesis. Catal Today.* (2005) vol. 106. pp. 170.

[10] Flynn C.M. Jr., Hydrolysis of inorganic iron (111) salts, J. Chem. Rev. (1984) vol. 84. pp. 31.

[11] Jean-Pierre J., Corinne C., Elisabeth T., Iron oxide chemistry. From molecular clusters to extended solid networks, J. Chem. Commun. (2004) vol. 481.

[12] Jean-Pierre J., Elisabeth T., Corinne C., Iron oxides: from molecular clusters to solid. *A nice example of chemical versatility, J. C.R. Geoscience*. (2006) vol. 338, pp. 488.

[13] Wagner R.M., Sandra H.P., Celso V.S., Aldo F.C., Formation of colloid particles of hydrous iron oxide by forced hydrolysis, *Journal of Non-Crystalline Solids*. (2000) vol. 273. pp. 41.

[14] Russo U., Carbonin S., Giusta A.D., in: Long G.J., Grandjean F. (Eds.), Mössbauer Spectroscopy Applied to Magnetism and Materials Science, Plenum, New York. (1996) vol. 2, pp. 207.

[15] Zhanbing H., Maurice J. L., Aurélien G., Chang S. L., Didier P., and Costel S. C., Iron Catalysts for the Growth of Carbon Nanofibers: Fe, Fe_3C or Both**, *Chem.* Mater.,(2011) vol. 23 (24), pp 5379–5387.

[16] Ibragimov Kh.D., Ismailov E.G., Martynova G.S., Bektashi N.R., Ibragimova Z.M., and Rustamov M.I., Synthesis of a Component of the Jet Engine Fuel and an Accelerator of Oil Tar Oxidation by Catalytic Processing of Heavy Pyrolysis Tar. *Russian Journal of Applied Chemistry*. (2010) vol. 83(7), pp. 1159-1163.

[17] Corma A., Navarro M., Perez-Pariente T., J. Chem. Soc. Chem. Commun. (1994) pp. 147–148.

[18] Wu M.B., Zha Q.F., Qiu J.S., Guo Y.S., Shang H.Y., Yuan A.J., Carbon. (2004) vol. 42. pp. 205. en University, the Mall, Rawalpindi, Pakistan, (2011).